A molecular phenology scale of fruit development

Giovanni Battista Tornielli[1*§], Marco Sandri[1,2§], Marianna Fasoli[1], Alessandra Amato[1], Mario Pezzotti[1], Paola Zuccolotto[2], Sara Zenoni[1]

[1] Department of Biotechnology, University of Verona, Strada Le Grazie 15, 37134, Verona, Italy

[2] Big & Open Data Innovation Laboratory, University of Brescia, C.da S. Chiara 50, 25122 Brescia, Italy

[§] These authors contributed equally to the manuscript

[*] Corresponding author

Abstract

Fruit growth and development consists of a continuous succession of physical, biochemical, and physiological changes driven by a genetic program that dynamically responds to environmental cues. Establishing recognizable stages over the whole fruit lifetime represents a fundamental requirement for research and fruit crop cultivation. This is especially relevant in perennial crops like the grapevine to scale the development of its fruit across genotypes and growing conditions. In this work, molecular-based information from several grape berry transcriptomic datasets was exploited to build a molecular phenology scale (MPhS) and to map the ontogenic development of the fruit. The proposed statistical pipeline consisted in an unsupervised learning procedure yielding an innovative combination of semiparametric, smoothing and dimensionality reduction tools. The transcriptomic distance between fruit samples was precisely quantified by means of the MPhS that also enabled to highlight the winding dynamics of the transcriptional program over berry development through the calculation of the rate of variation of MPhS stages by time. The MPhS allowed the alignment of time-series fruit samples proving to be a step forward in mapping the progression of grape berry development with higher precision compared to classic time- or phenotype-based approaches and inspiring the use of the transcriptional information to scale the developmental progression of any organ in any plant species.

Keywords

Molecular phenology, fruit development, transcriptional clock, grapevine, Bézier interpolation.

Introduction

The ontogenic development of fleshy fruits entails an ordered sequence of physical, chemical, physiological, and molecular changes that progressively drive the entire organ towards maturation. These processes are rather conserved among fruits of the same species, but the developmental progression may sway due to both genetic and environmental factors. Moreover, developmental expression patterns are extremely dynamic and, especially under fluctuating environmental conditions (Menzel et al., 2006; Nissanka et al., 2015; Alderman and Stanfill, 2017), rapid changes may happen within short time windows, challenging the setup of meaningful comparisons to study the fruit response to any factor. In annual or perennial fruit crops, the ontogenic development of the fruit is tracked by adopting phenological scales. These are classification tools to describe seasonal and precisely recognized stages of fruit growth and development based on specific descriptors such as visual/physical traits or easy-to-measure compositional parameters (Gillaspy et al., 1993; Labadie et al., 2019). Phenological scales are widely used in models describing known or hypothetical cause-effect relationships between growth stages progression and environmental driving factors (Hess, 1997; Parker et al., 2011; Parker et al., 2020).

In grapevine, the fruit phenophases comprise a large dedicated section of the most adopted phenology scales, namely the modified Eichhorn and Lorenz (E-L) (Coombe, 1995) and the extended BBCH systems (Lorenz et al., 1995), that assign increasing numbers to the main fruit developmental stages from setting to maturity. Grape berry development entails a curve consisting in two phases of growth and lasts up to 150 days (Coombe, 1992). The first phase (also called berry formation or herbaceous/green phase) involves pericarp growth due to rapid cell division and elongation. The second phase (ripening) involves physical and metabolic changes, including softening, skin pigmentation, accumulation of sugars, loss of organic acids, and synthesis of volatile aromas (Conde et al., 2007). The onset of ripening (veraison for viticulturists) occurs after a short lag phase, when the seeds maturation is complete (Coombe, 1992; Fasoli et al., 2018). Growth stages are defined by the assessment of visual/physical traits, such as color, size, and softness. Only for ripening stages and harvest decision, compositional

2

68   parameters like sugar concentration in the juice are considered. However, the precise definition

69   of developmental stages can be challenging as the fruit traits used for stage description are highly

70   influenced by several factors like genotype, climate, water availability, agronomical practices,

71   and crop load (Sadras and Moran, 2012; Parker et al., 2015; Pastore et al., 2017).

72   The advent of next-generation sequencing represents an opportunity to exploit the expression

73   kinetic of large sets of genes to stage the fruit development and enrich the available classification

74   systems incorporating information at molecular level (Chuine and Regniere, 2017; Gildor and

75   Smadar, 2018). This approach succeeded to develop a transcriptomic aging clock defining the

76   biological age of organisms such as *C. elegans* to an unprecedented accuracy (Meyer and

77   Schumacher, 2021) and, in plants, was used to reconstruct the transcriptional ontogeny of single

78   organs and correlate the appearance of morphological characteristics with molecularly defined

79   developmental stages (Leiboff and Hake, 2019). Moreover, results obtained on model organisms

80   such as Arabidopsis, or annual crops such as rice, revealed seasonal patterns of gene expression

81   controlled by environmental cues (Nagano et al., 2012; Nagano et al., 2019) and demonstrated

82   that the recent advancement of the methods for gene expression quantification could be exploited

83   to refine phenological stage classification (Kudoh, 2016).

84   The huge amount of transcriptomic studies generated in recent years over grape berry

85   development revealed that the variation of a portion of the fruit transcriptome is conserved across

86   cultivars and growing conditions (Fasoli et al., 2012; Dal Santo et al., 2013; Robinson et al.,

87   2015; Massonnet et al., 2017; Fasoli et al., 2018; Theine et al., 2021), and thus may be utilized to

88   boost the description of the fruit developmental stages with a molecular dimension.

89   In this work we used the most informative portion of several grapevine fruit transcriptomic

90   datasets (Massonnet et al., 2017; Fasoli et al., 2018) to build a molecular phenology scale

91   (MPhS). The performance of the scale in precisely mapping the progression of fruit

92   development, over other classical time- or phenotype-based approaches was assessed. The MPhS

93   was used to reinterpret previously published transcriptomic datasets evidencing its potential to

94   trace and compare fruit developmental stages from different genotypes and growing conditions.

95

96

Results

97

98 To create a molecular scale of grapevine berry development we relied on the RNA-sequencing

99 dataset consisting of 219 samples published by Fasoli et al. (2018). Samples were collected from

100 fruit set to full maturity from Cabernet Sauvignon (CS) and Pinot noir (PN) vines every 7–10

101 days across three years (Table S1).

102 Vintage variability impacted ripening progression since its onset that happened earlier in 2013

103 and 2014 compared to 2012, and then determined a substantial advance until the grape

104 technological maturity monitored by sugar accumulation (Fig. 1a,b). This behavior was more

105 evident in PN, an early ripening variety respect to CS.

106 Transcriptomic data was analyzed using statistical and data mining tools to define the core set of

107 genes marking the berry development progression (Fig. 1c). The pipeline comprised an initial

108 screening to discard genes exhibiting low and/or noisy expression that reduced the dataset from

109 29,971 to the whole core set (WCS) of 10,129 genes (Dataset S1), followed by the application of

110 a local polynomial regression that allowed smoothing the gene expression patterns over the time

111 points and averaging the replicates. We then performed Principal Component Analysis (PCA)

112 with the data matrix obtained by column-standardization of the smoothed gene expression. We

113 selected Principal Components (PCs) 1 and 2 that well described the general progression of berry

114 development, and PC5 that improved the discrimination of early stage samples (Fig. 1d),

115 whereas the effect of genotype and vintage (PC3, 4 and 6) was excluded (Fig. S1).The PCs

116 defined a three-dimensional scatter of points, with each point corresponding to an experimental

117 condition (one time point of one cultivar in one year) that were then fitted by one-dimensional

118 space using a Bézier curve. Thirty marks were evenly distributed along the curve to represent

119 steps of what we called Molecular Phenology Scale (MPhS) (Fig. 1e). The points of the 3D

120 scatter were projected onto the MPhS and assigned to the closest among the set of 30 marks,

121 demonstrating that the chronological order of all sampling series was maintained along the

122 MPhS (Fig. 1f), and the core gene set represented a suitable selection for our purpose.

123 The performances of the MPhS were next explored by projecting the non-smoothed three-year

124 time series of CS and PN on the MPhS. We found that the most part of the samples were

125 correctly ordered according to their chronological collection (Fig. 2a and Table S2). Four sample

126 pairs of CS mapped at the same MPhS stages and in two cases each genotype samples collected

127 at the beginning or at the end of series showed mapping discrepancy with the scale sequence,
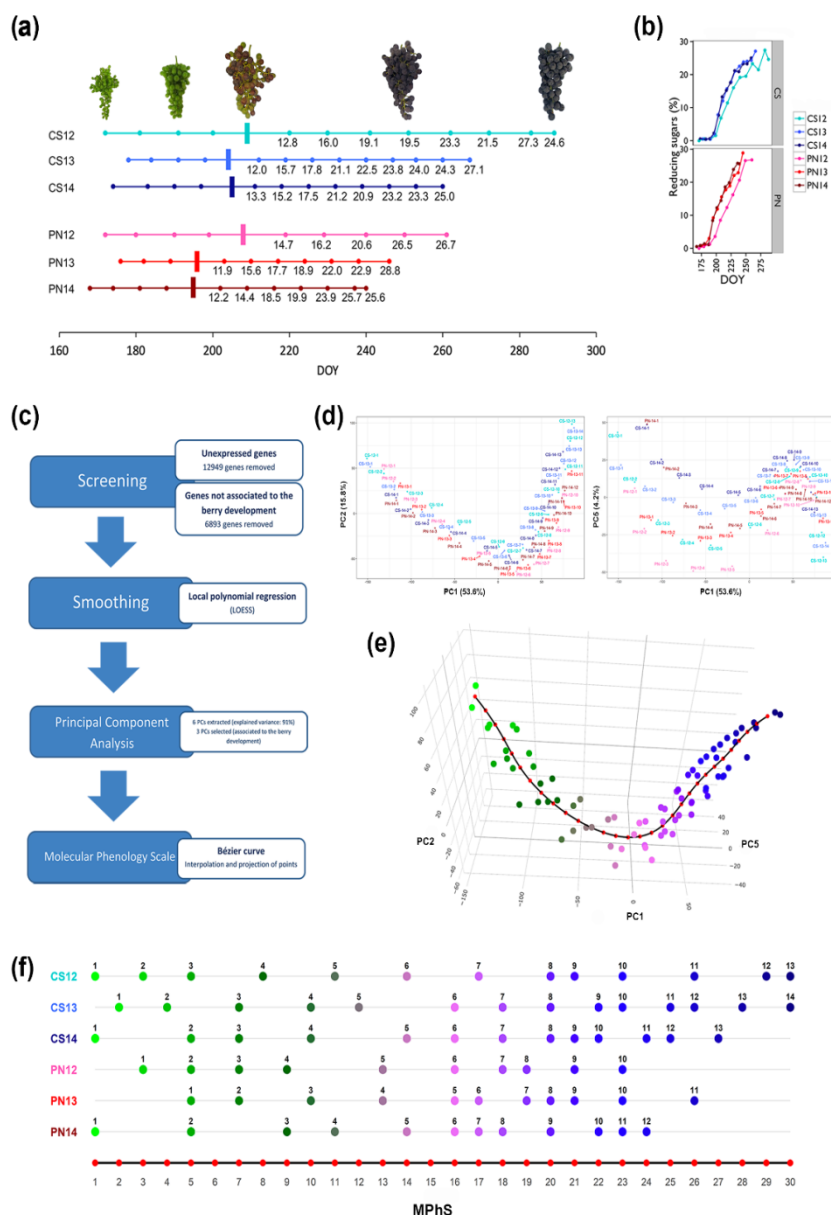
4

Fig. 1. Molecular phenology map creation.
(a) Cabernet Sauvignon and Pinot noir time series of berry sample collection. Berries were collected using a randomized block approach to account for intra-vineyard block variability. This resulted in a collection of 219 samples. Brix values are specified for time points post veraison (marked by vertical bar) along the timeline. Veraison: visually defined as the 50%-colored berry in the bunch. DOY, day of the year. Images on top show samples depicting five stages of grape cluster development for Cabernet Sauvignon during season 2012. (b) Accumulation trends of reducing sugars (%) by DOY in Cabernet Sauvignon and Pinot noir samples over three years. Plots were generated using R package ggplot2 version 2.2.1 (Wickham, 2009). DOY, day of the year. (c) Flow chart of the pipeline. The chart represents the four principal steps (blue rectangles) and related details (white rectangles) (d) Samples distribution according to the three selected PCs. PC1 (53.6%) by PC2 (15.8%) (left) and by PC5 (4.2%) (right). (e) Three-dimension scatterplot of the three selected PCs interpolated by the Bézier curve (black line). Red dots along the Bézier curve define a set of 30 evenly spaced molecular stages. Scattered points correspond to the smoothed samples and changing color highlight berry progression from immature to ripe stages. An interactive plot of the curve is accessible at the link https://bodai.unibs.it/grapevine-gea/mphs/. (f) Projection of the smoothed three-year time series of CS and PN to the closest point among the 30 points identified along the Bézier curve. The sample number is reported above each point. Red dots correspond to the 30 steps of the Molecular Phenology Scale.

128   suggesting a lower resolution of the MPhS at phases with reduced time-related transcriptomic
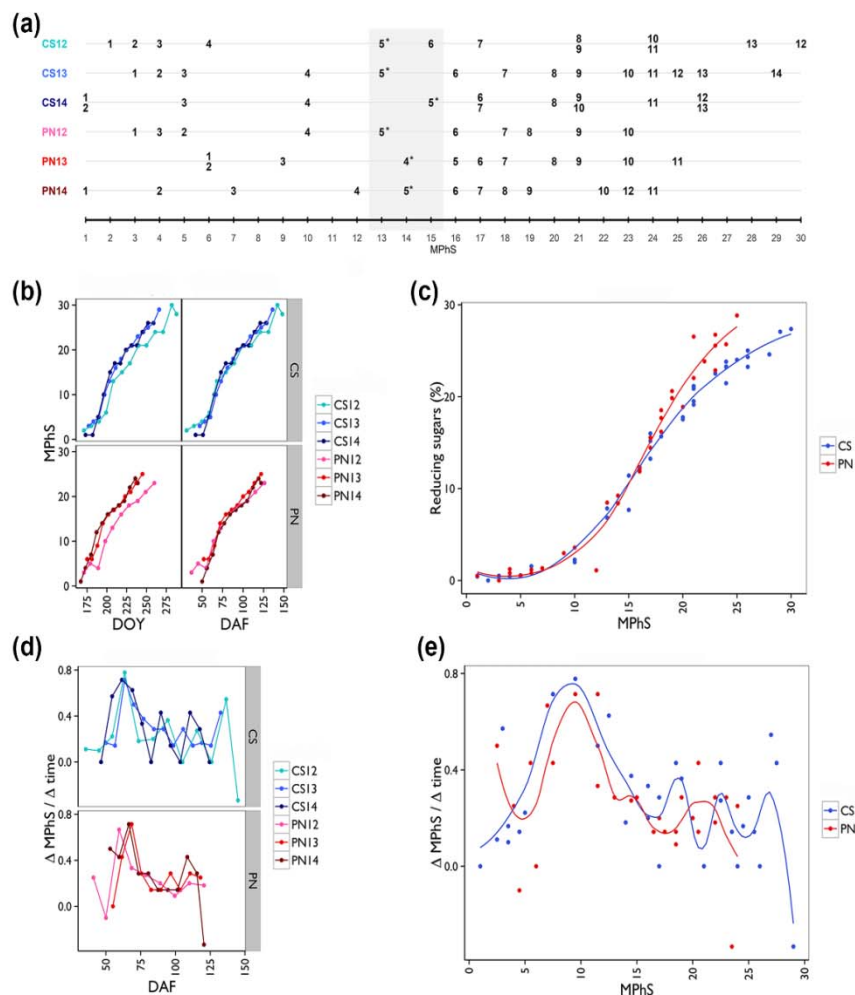
Fig. 2. Relationship between Molecular Phenology Scale and time during fruit development.
(a) Projection of the non-smoothed three-year time series of CS and PN on the MPhS. Samples collected at version phase are marked with an asterixis. The light-grey rectangle highlights the MPhS stages corresponding to the version transition. (b) Trends of MPhS stages by day of the year (DOY) (left) and day after flowering (DAF) (right) in CS and PN over the three years. Plots were generated using R package ggpplot2 version 2.2.1 (Wickham, 2009). (c) Trend of percentage of reducing sugars accumulation by MPhS in CS and PN. Smoothed conditional means function of the R package ggpplot2 version 2.2.1 (Wickham, 2009) was used to represent the average of the three years per genotype. (d) Plot of the ΔMPhS/Δtime over DAF. ΔMPhS represents the difference in MPhS between subsequent stages. Δtime represents the difference in days between subsequent stages. Plots were generated using R package ggpplot2 version 2.2.1 (Wickham, 2009). (e) Plot of the ΔMPhS/Δtime over the MPhS. Smoothed conditional means function of the R package ggpplot2 version 2.2.1 (Wickham, 2009) was used to represent the average of the three years per genotype.

129   changes. In fact, the samples were not evenly distributed along the MPhS and some intervals

130   (e.g., between MPhS stage 7 and 12) were poorly represented. The veraison phase was

131   pinpointed in correspondence to the MPhS window 13-15 for both genotypes, whereas PN

132   always reached maturity at earlier MPhS stage compared to CS.

133   Plotting the MPhS by the day of the year (DOY) confirmed differences among years and

134   evidenced a transcriptional progression delayed in 2012 in both varieties, whereas the alignment

135   on the phenological flowering phase resulted in nearly overlapping curves unraveling common

136   kinetics, with the very first phase characterized by slow transcriptional changes followed by a

137   rapid advancement clearly anticipating the veraison stage (Fig. 2b). Because similar dynamics

138   were observed when the MPhS series were plotted on the heat summation, we speculate that

139   temperature is less effective than time in driving fruit transcriptomic progression (Fig. S2).

140   When exploring the relation between MPhS stage and sugar content of the PN and CS samples,

141   we observed a strict non-linear relation that clearly varied in the two genotypes, with PN

142   reaching technological maturity at earlier MPhS stages than CS (Fig. 2c). On the other hand, an

143   elevated variability, beyond the clear genotype effect, was observed between MPhS and Berry

144   weight, suggesting that the two variables are poorly related (Fig. S3).

145   The transcriptomic scale dynamics highlighted by the ratio ΔMPhS/Δtime (an approximation of

146   the derivative of the MPhS curve over time) showed clear fluctuations irrespective of the DOY

147   (Fig. S4) and more aligned by genotype when plotted over the day after flowering (DAF),

148   evidencing a major peak likely associated with the onset of ripening, followed by some minor

149   peaks (Fig. 2d).

150   This dynamic was better highlighted by plotting the ΔMPhS/Δtime averaged by year over the

151   MPhS itself, revealing that some MPhS stages are rapidly passed through (Fig. 2e). A main burst

152   of speed was reached at stages 9-10 in both genotypes, followed by minor accelerations at stages

153   17-18, 22-23 and 27-28 in CS and around stage 22 in PN.

154   The performance of the MPhS was then tested on previously published berry transcriptomes by

155   mapping the relative samples onto the MPhS using the core set of 10,129 genes selected for the

156   scale definition.

157   The RNA-seq dataset from Massonnet et al. (2017) provided information in ten genotypes across

158   four berry phenological stages (BBCH scale) of the same season. When scaled onto the MPhS,

159   the two early stages, Pea Size and Touch, mapped nearby between stage 6 and 11 (Fig. 3a). Later

160   stages appeared less aligned across genotypes, spanning from the white-skin variety Passerina
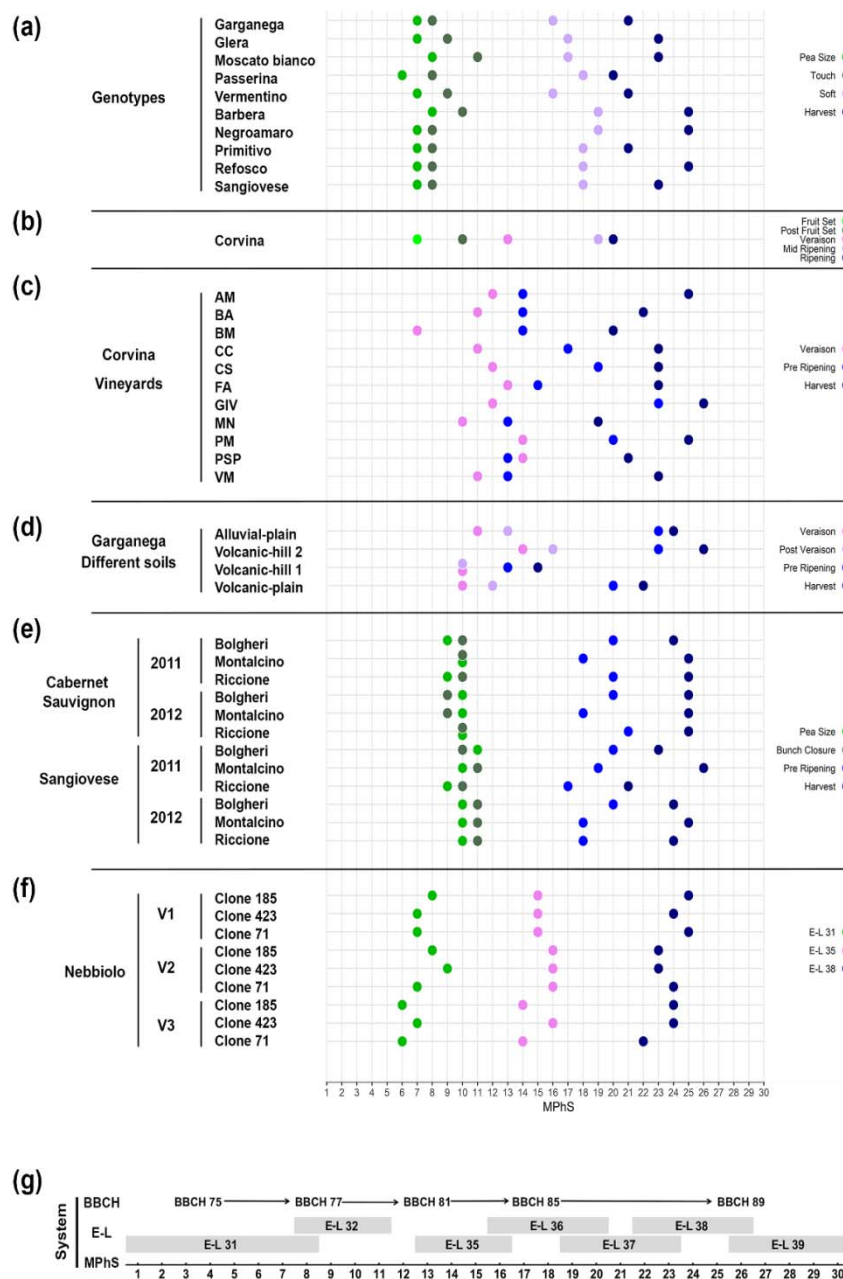
7

Fig. 3. Scaling of previously published berry transcriptomic samples onto the MPhS.
(a) Projection of RNA-seq transcriptomic berry samples of ten varieties (Massonnet et al., 2017) onto the MPhS. The BBCH scale was followed to collect berry samples at specific phenological stages: Pea Size (BBCH 75), Touch (BBCH 77), Soft (BBCH 85) and Harvest (BBCH 89) during the same season. (b) Projection of microarray transcriptomic berry samples of cv Corvina (Fasoli et al., 2012) onto the MPhS. Samples collection was performed at phenological stages defined by the E-L scale: Fruit Set (E-L 29), Post Fruit Set (E-L 32), Veraison (E-L 35), Mid Ripening (E-L 36) and Ripening (E-L 38). (c) Projection of microarray transcriptomic berry samples of cv Corvina collected at three ripening stages (Veraison, Pre Ripening and Harvest) from eleven cultivation sites (Dal Santo et al., 2013), onto the MPhS. (d) Projection of microarray transcriptomic berry samples of cv Garganega collected at four ripening stages (Veraison, Post Veraison, Pre Ripening and Harvest) from four cultivation sites (Dal Santo et al., 2016), onto the MPhS. (e) Projection of microarray transcriptomic berry samples of cv Sangiovese and cv Cabernet Sauvignon compared across three growing sites and over two years (Dal Santo et al., 2018), onto the MPhS. Berries were collected at four developmental stages defined by the BBCH phenological scale: Pea Size (BBCH 75), Bunch Closure (BBCH 79), Pre Ripening (BBCH 83) and Harvest (BBCH 89). (f) Projection of RNA-seq transcriptomic berry samples of three clones of cv Nebbiolo, compared across three different sites (Pagliarani et al., 2019), onto the MPhS. Samples were collected at three developmental stages defined by the E-L phenological scale: Pea Size (E-L 31), Veraison (E-L 35), and Ripening (E-L 38). We represented seven main stages in the legend: stage 1 (Fruit Set and E-L 29; light green), stage 2 (Pea Size and E-L 31; green), stage 3 (Touch, Post Fruit Set, Bunch Closure and E-L 32; olive green), stage 4 (Veraison and E-L 35; pink), stage 5 (Soft, Mid Ripening, Post Veraison and E-L 36; plum), stage 6 (Pre Ripening and E-L 37; blue) and stage 7 (Harvest, Ripening and E-L 38, midnight blue). (g) Alignment between MPhS and two phenotype-based phenological scales (BBCH and the modified E-L) during berry development.

161   that mapped at MPhS stage 20 at Harvest, to the red-skin Barbera, Negroamaro and Refosco,

8

162 exhibiting maturity at 25.

163 We also scaled samples from microarray-based transcriptomic datasets among which the five

164 phenological stages (E-L scale) of the cultivar Corvina (Fasoli et al., 2012). Albeit obtained by a

165 different transcriptomic technology, samples mapped neatly onto the MPhS, with green berry

166 samples projected at stage 7 and 10, Veraison at stage 13, whereas Mid Ripening and Ripening at

167 stages 19 and 20, respectively (Fig. 3b).

168   A benefit of the molecular scale consists in recalibrating studies that organized sampling on a

169 time-based approach rather than following berry phenology. This was the case of two

170 microarray-based transcriptomic datasets in which berries of the cultivar Corvina were collected

171 at three ripening times from eleven sites (Dal Santo et al., 2013), whereas for the cultivar

172 Garganega they were collected at four ripening times from four sites (Dal Santo et al., 2016). As

173 expected, datasets projection onto the MPhS revealed a fair misalignment of time points

174 collected from different sites (Fig. 3c,d). The greatest differences were observed for Corvina

175 samples at the second stage ranging from MPhS stage 13 to 23, whereas Garganega berries

176 mapped between MPhS stage 15 and 26 at harvest.

177 Mapping samples from the work of Dal Santo and co-authors (2018), exploring the genotype by

178 environment interaction (GxE), revealed that berries of the cultivar Sangiovese reached maturity

179 at different MPhS stages by cultivation site and year whereas Cabernet Sauvignon samples

180 appeared much more aligned (Fig. 3e) affirming the marked transcriptomic plasticity of

181 Sangiovese. The strength of the MPhS mapping approach to GxE was also assessed when the

182 genotype component represented different clones, like in the work of Pagliarani et al. (2019)

183 entailing RNA-seq berry samples of three clones of the cultivar Nebbiolo, grown in three sites,

184 and collected at three developmental stages. Although samples arranged along the MPhS by E-L

185 phenological classification (Fig. 3f), minor MPhS shifts reflecting the intrinsic transcriptomic

186 plasticity of each clone interacting with the growing site were yet appreciable.

187 The available sampling metadata was then exploited to attempt an alignment between our MPhS

188 and the classical phenotype-based phenological scales (i.e., the modified E-L and BBCH

189 systems) during berry development (Fig. 3g), showing the greater classification detail provided

190 by the MPhS compared to the traditional scales.

191   Starting from the core set of genes used to create the MPhS, we next focused on identifying the

192   smallest number of genes necessary to efficiently map berry transcriptomic samples onto the

193   MPhS.

194   Pools of 20, 10, 5 and 2 positive and negative loadings of each of the three PCA components

195   (corresponding to 120, 60, 30 and 12 genes, respectively) were selected based on their absolute

196   correlation value (p-corr) and expression profile. Hierarchical cluster analysis of the top-100

197   loadings throughout berry development in PN and CS during the three vintages revealed 20 main

198   clusters of gene expression (Fig. S5). As genes belonging to the same metabolic/developmental

199   process likely co-express, we picked genes with high p-corr value from each cluster to maximize

200   the information potential thus avoiding redundancy (Dataset S2). Calculating the average shift

201   between the projections of the sample series defined by the reduced core sets (RCS) and the

202   WCS allowed evaluating any difference in performance (Fig. 4). This analysis highlighted that

203   the progressive reduction of the core gene set from 120 to 12 did not substantially impacted the

204   samples order along the MPhS and only slightly worsened its scaling performance.
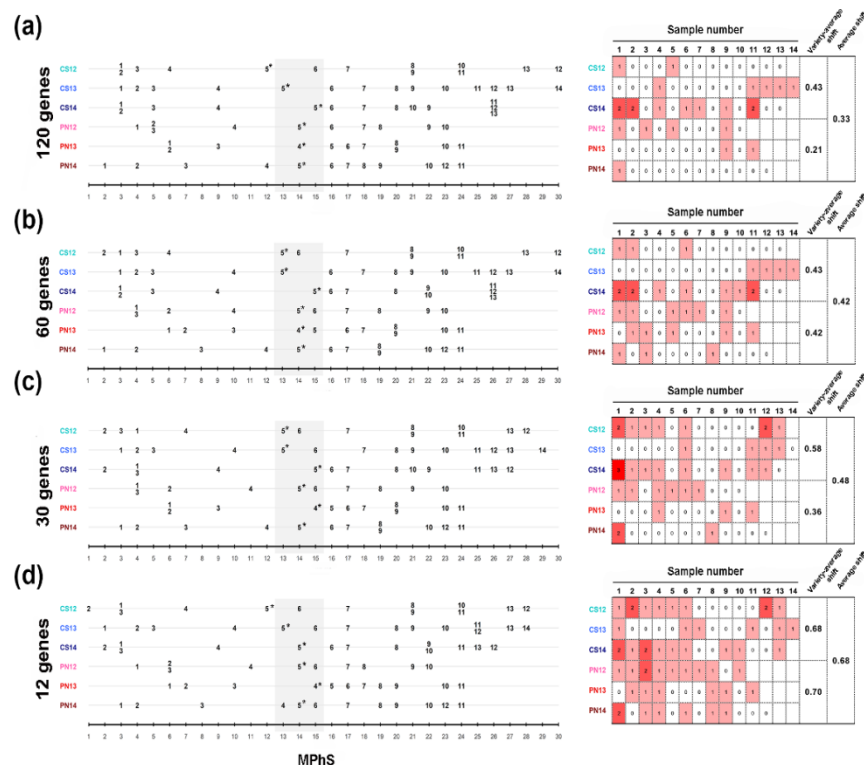
205

206

Fig. 4. Performance of MPhS based on a reduced core set of genes.
Projections of the sample series defined by the progressively reduced core set of genes (a) 120 genes, (b) 60 genes, (c) 30 genes and (d) 12 genes (Dataset S2) onto the MPhS (left) and representation of the average shifts between the distribution of samples defined by reduced core sets versus when defined by the entire core set of genes (10,129) (right). For each sample the shift between the MPhS stage defined by the reduced gene core set and the MPhS stage defined by the entire gene core set was calculated. The overall and by variety average shift are shown per reduced core set of genes.

207　**Discussion**

11

208 Assembling meaningful comparisons between fruits characterized by different developmental
209 rates or seasonal developmental shifts is a major limitation in studying the biological
210 mechanisms underpinning the seamless developmental progression that leads the fruit to
211 maturation. The opportunity of refining the existing development classification systems by
212 integrating phenotype with molecular-based information has been explored in model organisms
213 or annual crops (Kudoh, 2016; Nagano et al., 2019; Meyer and Schumacher, 2021). The
214 transcriptomic analysis of immature maize tassels and sorghum panicles throughout development
215 enabled reconstructing their transcriptional ontogeny and correlating the emergence of species-
216 specific morphological characteristics of these organs to developmental stages defined at
217 molecular level (Leiboff and Hake, 2019). Despite omics technologies have been widely applied
218 to unveil and describe in detail the ongoing developmental changes in fleshy fruits from many
219 species (Janssen et al., 2008; Sanchez-Sevilla et al., 2017; Fasoli et al., 2018; Shinozaki et al.,
220 2018), the molecular information was rarely exploited to attempt at scaling the fruit ontogeny. In
221 grapevine, Dai et al. (2013) demonstrated that metabolite profiling can be used in PCAs to define
222 development trajectories for berries, whereas Wang et al. (2014) showed that the expression
223 trend of a small number of genes involved in grapevine flower and berry development was
224 associated to some specific phenological stages. In this study, we selected about ten thousand
225 genes from several transcriptomic datasets for their consistent expression throughout berry
226 development regardless genotype and season (Massonnet et al., 2017; Fasoli et al., 2018) and
227 built a molecular phenology scale to map the ontogenetic development of the fruit with high
228 precision and to align berry development of different grapes. The proposed statistical pipeline
229 consisted in an unsupervised learning procedure yielding an innovative combination of
230 semiparametric, smoothing and dimensionality reduction tools. Time information was exploited
231 by only considering timepoints succession disregarding their distance so the MPhS units are not
232 time but ideal steps of the berry development, which can take longer or shorter, providing the
233 flexibility of accounting for a multiplicity of factors. Additionally, it is worth mentioning that the
234 Principal Components were exceptionally able to summarize different characteristics of the data
235 (berry variety, vintage, stage) allowing to precisely select genes involved in berry development
236 and rule out those impacted by genotype and vintage.
237 When projecting onto the MPhS the sample series used for its own constructions, the distribution
238 was largely by the time of collection during the season, with very few overlaps or inversions.

239 These cases were mainly concentrated at the initial and final stages of the scale suggesting that
240 berry transcriptome evolution right after fruit set and near maturity is slower than during the
241 central time frame, therefore samples collected at two consecutive weeks could exhibit very
242 similar transcriptomes. Indeed, the uneven distribution of samples along the scale mirrored the
243 winding dynamics of berry transcriptome over development revealing that some MPhS stages are
244 more rapidly crossed by the developing fruit. For both varieties the highest rate of variation of
245 the MPhS stage by time (represented by a major peak) was recorded well prior the assessed
246 veraison stage, confirming that the ripening transcriptional program is established one-to-two
247 weeks before berry phenotypic changes can be visually appreciated (Castellarin et al., 2016;
248 Fasoli et al., 2018; Hernández-Montes et al., 2021). Following the onset of ripening, minor peaks
249 were present towards maturity suggesting that the ripening progression is discontinuous at
250 transcriptional level. We exclude these fluctuations to be caused by interactions with the
251 environment as the statistical pipeline was set to screen out the vintage component and any
252 erratic variation of gene expression.

253 Applications of the MPhS are aligning samples to highlight shifts of fruit development driven by
254 factors like genotype and environment as well as precisely quantifying their transcriptomic
255 distance. This could represent a start to pinpoint the specific contribution of any variance in fruit
256 development and the cultivation environment to the overall plasticity. Once fruit samples align
257 by MPhS stage, comparing differentially expressed genes could unveil responses uniquely
258 related to the growing conditions. Projecting RNA-seq and microarray transcriptomic samples
259 (Fasoli et al., 2012; Dal Santo et al., 2013; Dal Santo et al., 2016; Massonnet et al., 2017; Dal
260 Santo et al., 2018; Pagliarani et al., 2019) onto the MPhS indeed highlighted phenological
261 differences and provided the basis to shed the light into instances when samples originally
262 assigned to similar phenological stage mapped relatively apart along the MPhS. Nevertheless, the
263 MPhS ability to discriminate samples collected at a considerable time distance was not fully
264 confirmed in certain dataset/time series. This may be related to specific raw data processing and
265 procedures adopted in each study, prompting the need of future investigation and development of
266 broader normalization protocols to improve the performance of the MPhS.

267 Regarding the classification of ripening stage, the molecular scale represents an advance over the
268 traditional analytical methods (i.e., total soluble solids or reducing sugars percentage in the grape
269 juice) that, although rapid, do not always represent a reliable indicator of the berry physiological

270   ripening stage. In fact, the great influence of genetics, climate, and agronomic factors on sugar
271   accumulation dynamics in the fruit can lead to a partial uncoupling from other ripening
272   technological parameters, like organic acids and skin pigment content (Sadras and Moran, 2012;
273   Parker et al., 2015; Pastore et al., 2017). We found a close relation between MPhS stage and
274   berry sugar level at initial stages of maturation in both cultivars, that diverged at late maturation
275   likely reflecting the different length of ripening characterizing the two genotypes and indicating
276   that CS berries reached the target level of soluble solids at an advanced MPhS stage compared to
277   PN.

278   Based upon the metadata available for each dataset, we attempted to approximate the 1-30 MPhS
279   stages to those specified in the classical grapevine fruit phenology scales and we thus attested
280   that the MPhS permits greater definition of the phenophases respect to the classical scales
281   (Coombe, 1995; Lorenz et al., 1995) that cover longer stretches along berry development.

282   Finally, we showed that the number of expression signals necessary for mapping samples on the
283   MPhS can be drastically reduced to a few dozen without substantial loss of precision, creating
284   the opportunity of defining the molecular phenology stage of a fruit sample just performing
285   targeted gene expression analysis.

286   The proposed scale paves the way for the development of tools that aspire at predicting the
287   phenological stage of the fruit in various climate conditions, such as models that can account for
288   temperature and other environment clues. The quality of these tools will benefit from the
289   combination of various modeling techniques (molecular, metabolite, physical, visual levels),
290   providing that great coordination and knowledge-transfer between modelers, biologists and
291   growers will be established.

292   The proposed pipeline could be potentially extended and successfully applied to any other fruit
293   species, provided they have some basic requirements: (i) a relatively frequent sampling covering
294   the time-series transcriptomic changes during fruit development with high detail; (ii) the
295   availability of expression data from diverse growing conditions and genotypes allowing the
296   phenology scale to be representative of the general development of the fruit of the species; (iii) a
297   reliable and well annotated reference genome to compute the expression data. The existence of
298   these conditions ensured the successful implementation of our MPhS for the grapevine berry
299   phenological classification, that we foresee will help coping with challenges such as those raised
300   by climate change, allowing the precise mapping of the berry developmental progression.

301

Materials and Methods

Transcriptomic datasets

The expression data used for the creation of MPhS was retrieved from Fasoli et al. (2018) (data accession number GSE98923), whereas the berry transcriptomes projected onto the MPhS referred to: Massonnet et al. (2017) (data accession number GSE62744 and GSE62745); Fasoli et al. (2012) (data accession number GSE36128), Dal Santo et al. (2013) (data accession number GSE41633); Dal Santo et al. (2016) (data accession number GSE75565); Dal Santo et al. (2018) (data accession number GSE97578); Pagliarani et al. (2019) (data accession number GSE116238).

Data mining process

We used the data described in Fasoli et al. (2018) (*dataset A*) and set the following variables:

- Cultivar [Cabernet Sauvignon, Pinot Noir]
- Vintage [2012, 2013, 2014]
- Timepoint [from 1 to 10-14 (different combinations Cultivar x Vintage have different final Timepoints)]

CxV denotes the six possible combinations Cultivar x Vintage and the term *experimental condition* represents each of the 73 possible combinations Cultivar x Vintage x Timepoint.

Genetic Variables:

- Gene Expression [RNAseq platform]

x_{jri} denotes the expression of gene i (i=1, 2, …, 29,971) in the jth experimental condition (j=1, 2, …, 73) for the rth replicate (r=1, 2, 3); the subscript h represents the combination CxV (h=1, 2, …, 6). J_h denotes the set of experimental conditions corresponding to $CxV = h$.

In addition, m_{ji} indicates the average expression (over the three replicates) of gene i in the jth experimental condition

$$m_{ji} = \frac{1}{3}\sum_{r=1}^{3} x_{jri}$$

15

327 and m_{hi} the average expression (over the replicated and the timepoints) of gene i in the hth CxV

328 combination

$$m_{hi} = \frac{1}{3|J_h|} \sum_{r=1}^{3} \sum_{j \in J_h} x_{jri}$$

329 where $|\cdot|$ denotes cardinality of a set.

330 Th expression profiles of each gene were displayed using a three-panel graphical representation

331 (Fig. S6), with one graph each vintage.

332 The data mining process comprises four steps (Fig. S7):

Step 1: Screening

334 We removed 19,842 genes from the 29,971 in the grapevine transcriptome exhibiting

335 uninteresting profiles (i.e., no expression in some experimental conditions or expression not

336 associated to berry development; Fig. S8) based on the criteria summarized in Table S3. To

337 improve the selection, this screening step exploited the information of an additional dataset

338 (*dataset B*), composed of 10 cultivars, observed for 4 timepoints during fruit development in a

339 single vintage (Massonnet et al., 2017). The resulting dataset comprised 10,129 genes (denoted

340 as *F*) deserving further statistical analysis.

Step 2: Smoothing

342 Smoothing was applied to the data matrix (219 x 10,129) containing the expressions x_{jri} with

343 $i \in F$. For each gene i and for each CxV combination h, we estimated smoothed values $\bar{x}_{ji}$ by

344 means of a polynomial local regression method called LOESS, introduced by Cleveland (1979)

345 and Cleveland and Devlin (1988). LOESS fits a low-degree polynomial to a subset of the data in

346 the neighborhood of each observation of the dataset. In other words, simple parametric models

347 are fitted to localized subsets of the data, aiming at obtaining a smooth curve. The polynomial

348 parameters are estimated by a weighted least squares method, where a higher weight is given to

349 points closer to the observation whose outcome is being calculated. The fraction of the total

350 number of data points that were used in each local fit is determined by the smoothing parameter,

351 usually denoted by α.

352 In the context of this application, for a gene i, the single observation was the expression of

353 replicate r of a given cultivar, in a given vintage, at a given timepoint. The neighborhood was

16

354   composed of all the expressions of gene *i*, for the same cultivar and in the same vintage, in the

355   nearby timepoints, with higher weights to the closest ones. We used polynomials of degree 2 and

356   set α = 0.75. The outcome $\bar{x}_{ji}$ for the experimental condition $j \in J_h$ was then calculated by

357   evaluating the local polynomial at the timepoint characterizing the experimental condition.

358   For each gene, a three-panel graphical representation could be visualized, analogous to that

359   presented in Fig. S6, where, in each panel, the line shows the pattern of the smoothed gene

360   expression $\bar{x}_{ji}$ (Fig. S9).

361   **Step 3: Principal Component Analysis**

362   This step was applied to the data matrix (73 x 10,129) containing the smoothed expressions $\bar{x}_{ji}$

363   with $\in F$. We performed PCA (Jolliffe, 1986) on the standardized data matrix and extracted six

364   PCs accounting for a 91% explained variance. The interpretation of the PCs was based on the

365   graphical representations in Fig. S10, where the pattern of each PC was plotted against the

366   timepoints, with lines corresponding to the different *CxV* combinations.

367   **Step 4: Molecular Phenology Scale definition**

368   This step concerned the data matrix (73 x 3) containing the values of PC1, PC2 and PC5 for each

369   experimental condition, which can be represented as a scatter of points in a three-dimensional

370   Euclidean space, with the implicit additional information of a timeline expressed by the

371   timepoints and the calendar day. The scatter of points was interpolated by means of a Bézier

372   curve (Rabut, 2002), which nowadays is employed in several applications, especially in the field

373   of computer graphics. A Bézier curve aims at fitting points with a smooth curve completely

374   contained within the convex hull of a set of *k* control points (*k* is called the curve's order): the

375   first and last control points are the end points of the curve, whereas the curve does not pass

376   through the intermediate ones (if any), which define orientation and shape.

377   In the context of our application, we set *k* = 5 and obtained the curve in Fig. S11. An interactive

378   plot of the curve is accessible at the link https://bodai.unibs.it/grapevine-gea/mphs/.

379   We projected the scatter on the Bézier curve by assigning each point of the scatter to the closest

380   point among a set of 30 evenly spaced points identified along the Bézier curve. We represented

381   the curve as a linear graduation, called Molecular Phenology Scale. Each experimental condition

17

382   was assigned to one of the 30 marks and the Molecular Phenology Scale was represented for

383   each CxV combination h, thus showing on the map only the experimental conditions $j \in J_h$.

384

Projection of transcriptomic data on the MPhS

386   In this section we describe the procedure to project observations coming from different case

387   studies onto the Molecular Phenology Scale. We used the matrix A of the eigenvectors of the

388   three selected Principal Components used to build the Molecular Phenology Scale.

389   Let $Z_{obs} = \{z_{ji}\}$ be a $|J_{obs}|$ x $|I_{obs}|$ data matrix containing the observed expression levels of a

390   set I_{obs} of genes for a set J_{obs} of experimental conditions, where $j = 1, 2, \cdots, |J_{obs}|$ and $i =$

391    $1, 2, \cdots, |I_{obs}|$. The matrix Z_{obs} was column standardized. We consider two cases:

392   1. $F \subseteq I_{obs}$ (recall that F is the set of 10,129 selected genes after the screening step).

393   In this case we obtained the matrix $\tilde{Z}_{obs} = \{z_{ji}\}$ $(j = 1,2, \cdots, |J_{obs}|$ and

394            $i = 1,2, \cdots, 10129)$ by removing from Z_{obs} the columns not belonging to F. Using

395            $Y_{obs} = \tilde{Z}_{obs} \cdot A$ we obtained the estimates of the three Principal Component values for the

396   observed values of the $|J_{obs}|$ experimental conditions;

397   2. $I_{obs} \subset F$.

398   This case typically occurs when a limited number of genes is observed, for example for

399   cost reasons. When this is the case, it is recommended to observe genes highly correlated

400   to the Principal Components, that should help obtaining good estimates in spite of the

401   scarcity of data.

402   Starting from the matrix Z_{obs} containing the observations of a limited number of genes

403            $|I_{obs}|$, we obtained the estimates of the Principal Component values for the observed

404   values of the $|J_{obs}|$ experimental conditions as follows:

405   • we computed the average expressions of the $|I_{obs}|$ genes positively and negatively

406   correlated to each Principal Component;

407   • for Principal Component q, we imputed the missing data (non-observed expressions

408   for genes in F) with the respective positive or negative average, according to the sign

409   of the corresponding eigenvector coefficient;

18

410 • let this imputed $|J_{obs}| \times 10129$ matrix be denoted with $Z_{obs,q}$, we obtained the

411 estimates of Principal Component q as $Y_{obs,q} = Z_{obs,q} \cdot A_q$, where A_q was the q-th

412 column of A.

413 Once obtained the estimates of the three Principal Component values, we plotted the estimated

414 three-dimensional scatter. This cloud of points was then projected onto the Bézier curve

415 estimated in step 4 by assigning each point to its closest marker among the set of 30 evenly

416 spaced points previously identified along the curve.

417

418 **Selection of transcripts for the reduced core set-based scale**

419 We investigated four scenarios in case 2 $(I_{obs} \subset F)$, characterized by different subsets of genes

420 with |I_obs |=120, 60, 30, 12, respectively. For the selection of 120, 60, 30, 12 genes, the

421 expression profile of the top-100 loadings characterized by the highest and lowest correlation

422 values with the three dimensions of the PCA were hierarchically clustered based on average

423 Pearson's distance metric (Tmev 4.3). We selected genes from each of the 20 different clusters.

424 Genes with the highest p-corr value within a cluster were preferred. For the PC5 the selection

425 was based only on the p-core values given their general low levels.

426

427 **Acknowledgments**

428 This work is based upon work from COST Action CA17111 INTEGRAPE, supported by COST

429 (European Cooperation in Science and Technology).

430

431 **Author contributions**

432 GBT and SZ conceived the research; GBT, MS, PZ and SZ designed the experiments; MS, PZ

433 and MF performed experiments; MS, PZ, MF, GBT and SZ analysed data; GBT, MS, PZ, SZ,

434 MF interpreted data; MP and AA helped drafting the manuscript; GBT, SZ and MF wrote the

435 manuscript; GBT and MS contributed equally.

436
437 **Figure Legends**
438
439 **Fig. 1. Molecular phenology map creation.**

440   (a) Cabernet Sauvignon and Pinot noir time series of berry sample collection. Berries were

441   collected using a randomized block approach to account for intra-vineyard block variability. This

442   resulted in a collection of 219 samples. Brix values are specified for time points post veraison

443   (marked by vertical bar) along the timeline. Veraison: visually defined as the 50%-colored berry

444   in the bunch. DOY, day of the year. Images on top show samples depicting five stages of grape

445   cluster development for Cabernet Sauvignon during season 2012. (b) Accumulation trends of

446   reducing sugars (%) by DOY in Cabernet Sauvignon and Pinot noir samples over three years.

447   Plots were generated using R package ggpplot2 version 2.2.1 (Wickham, 2009). DOY, day of the

448   year. (c) Flow chart of the pipeline. The chart represents the four principal steps (blue rectangles)

449   and related details (white rectangles) (d) Samples distribution according to the three selected

450   PCs. PC1 (53.6%) by PC2 (15.8%) (left) and by PC5 (4.2%) (right). (e) Three-dimension

451   scatterplot of the three selected PCs interpolated by the Bézier curve (black line). Red dots along

452   the Bézier curve define a set of 30 evenly spaced molecular stages. Scattered points correspond

453   to the smoothed samples and changing color highlight berry progression from immature to ripe

454   stages. An interactive plot of the curve is accessible at the link https://bodai.unibs.it/grapevine-

455   gea/mphs/. (f) Projection of the smoothed three-year time series of CS and PN to the closest

456   point among the 30 points identified along the Bézier curve. The sample number is reported

457   above each point. Red dots correspond to the 30 steps of the Molecular Phenology Scale.

458

459   **Fig. 2.**   **Relationship between Molecular Phenology Scale and time during fruit**

460   **development.**

461   (a) Projection of the non-smoothed three-year time series of CS and PN on the MPhS. Samples

462   collected at version phase are marked with an asterixis. The light-grey rectangle highlights the

463   MPhS stages corresponding to the version transition. (b) Trends of MPhS stages by day of the

464   year (DOY) (left) and day after flowering (DAF) (right) in CS and PN over the three years. Plots

465   were generated using R package ggpplot2 version 2.2.1 (Wickham, 2009). (c) Trend of

466   percentage of reducing sugars accumulation by MPhS in CS and PN. Smoothed conditional

467   means function of the R package ggpplot2 version 2.2.1 (Wickham, 2009) was used to represent

468   the average of the three years per genotype. (d) Plot of the ΔMPhS/Δtime over DAF. ΔMPhS

469   represents the difference in MPhS between subsequent stages. Δtime represents the difference in

470   days between subsequent stages. Plots were generated using R package ggpplot2 version 2.2.1

471 (Wickham, 2009). (e) Plot of the ΔMPhS/Δtime over the MPhS. Smoothed conditional means

472 function of the R package ggpplot2 version 2.2.1 (Wickham, 2009) was used to represent the

473 average of the three years per genotype.

474

475 **Fig. 3. Scaling of previously published berry transcriptomic samples onto the MPhS.**

476 (a) Projection of RNA-seq transcriptomic berry samples of ten varieties (Massonnet et al., 2017)

477 onto the MPhS. The BBCH scale was followed to collect berry samples at specific phenological

478 stages: Pea Size (BBCH 75), Touch (BBCH 77), Soft (BBCH 85) and Harvest (BBCH 89)

479 during the same season. (b) Projection of microarray transcriptomic berry samples of cv Corvina

480 (Fasoli et al., 2012) onto the MPhS. Samples collection was performed at phenological stages

481 defined by the E-L scale: Fruit Set (E-L 29), Post Fruit Set (E-L 32), Veraison (E-L 35), Mid

482 Ripening (E-L 36) and Ripening (E-L 38). (c) Projection of microarray transcriptomic berry

483 samples of cv Corvina collected at three ripening stages (Veraison, Pre Ripening and Harvest)

484 from eleven cultivation sites (Dal Santo et al., 2013), onto the MPhS. (d) Projection of

485 microarray transcriptomic berry samples of cv Garganega collected at four ripening stages

486 (Veraison, Post Veraison, Pre Ripening and Harvest) from four cultivation sites (Dal Santo et al.,

487 2016), onto the MPhS. (e) Projection of microarray transcriptomic berry samples of cv

488 Sangiovese and cv Cabernet Sauvignon compared across three growing sites and over two years

489 (Dal Santo et al., 2018), onto the MPhS. Berries were collected at four developmental stages

490 defined by the BBCH phenological scale: Pea Size (BBCH 75), Bunch Closure (BBCH 79), Pre

491 Ripening (BBCH 83) and Harvest (BBCH 89). (f) Projection of RNA-seq transcriptomic berry

492 samples of three clones of cv Nebbiolo, compared across three different sites (Pagliarani et al.,

493 2019), onto the MPhS. Samples were collected at three developmental stages defined by the E-L

494 phenological scale: Pea Size (E-L 31), Veraison (E-L 35), and Ripening (E-L 38). We

495 represented seven main stages in the legend: stage 1 (Fruit Set and E-L 29; light green), stage 2

496 (Pea Size and E-L 31; green), stage 3 (Touch, Post Fruit Set, Bunch Closure and E-L 32; olive

497 green), stage 4 (Veraison and E-L 35; pink), stage 5 (Soft, Mid Ripening, Post Veraison and E-L

498 36; plum), stage 6 (Pre Ripening and E-L 37; blue) and stage 7 (Harvest, Ripening and E-L 38,

499 midnight blue). (g) Alignment between MPhS and two phenotype-based phenological scales

500 (BBCH and the modified E-L) during berry development.

501

502 **Fig. 4. Performance of MPhS based on a reduced core set of genes.**

503 Projections of the sample series defined by the progressively reduced core set of genes (a) 120

504 genes, (b) 60 genes, (c) 30 genes and (d) 12 genes (Dataset S2) onto the MPhS (left) and

505 representation of the average shifts between the distribution of samples defined by reduced core

506 sets versus when defined by the entire core set of genes (10,129) (right). For each sample the

507 shift between the MPhS stage defined by the reduced gene core set and the MPhS stage defined

508 by the entire gene core set was calculated. The overall and by variety average shift are shown per

509 reduced core set of genes.

510

22

511

Parsed Citations

Alderman PD, Stanfill B (2017) Quantifying model-structure- and parameter-driven uncertainties in spring wheat phenology prediction with Bayesian analysis. European Journal of Agronomy 88: 1-9
  Google Scholar: Author Only Title Only Author and Title

Castellarin SD, Gambetta GA, Wada H, Krasnow MN, Cramer GR, Peterlunger E, Shackel KA, Matthews MA (2016) Characterization of major ripening events during softening in grape: turgor, sugar accumulation, abscisic acid metabolism, colour development, and their relationship with growth. J Exp Bot 67: 709-722
  Google Scholar: Author Only Title Only Author and Title

Chuine I, Regniere J (2017) Process-Based Models of Phenology for Plants and Animals. Annual Review of Ecology, Evolution, and Systematics, Vol 48 48: 159-182
  Google Scholar: Author Only Title Only Author and Title

Cleveland DW (1979) Robust locally weighted regression and smoothing scatterplots. Journal of the American Statistical Association 74
  Google Scholar: Author Only Title Only Author and Title

Cleveland DW (1988) Locally weighted regression: an approach to regression analysis by local fitting. Journal of the American Statistical Association 83
  Google Scholar: Author Only Title Only Author and Title

Conde C, Silva P, Fontes N, Dias ACP, Tavares RM, Sousa MJ, Agasse A, Delrot S, Gerós H (2007) Biochemical changes throughout grape berry development and fruit and wine qua. Food 1: 22
  Google Scholar: Author Only Title Only Author and Title

Coombe BG (1992) Research on Development and Ripening of the Grape Berry. American Journal of Enology and Viticulture 43: 101-110
  Google Scholar: Author Only Title Only Author and Title

Coombe BG (1995) Adoption of a system for identifying grapevine growth stages. Australian Journal of Grape and Wine Research 1: 10
  Google Scholar: Author Only Title Only Author and Title

Dai ZW, Leon C, Feil R, Lunn JE, Delrot S, Gomes E (2013) Metabolic profiling reveals coordinated switches in primary carbohydrate metabolism in grape berry (Vitis vinifera L.), a non-climacteric fleshy fruit. J Exp Bot 64: 1345-1355
  Google Scholar: Author Only Title Only Author and Title

Dal Santo S, Fasoli M, Negri S, D'Inca E, Vicenzi N, Guzzo F, Tornielli GB, Pezzotti M, Zenoni S (2016) Plasticity of the Berry Ripening Program in a White Grape Variety. Front Plant Sci 7: 970
  Google Scholar: Author Only Title Only Author and Title

Dal Santo S, Tornielli GB, Zenoni S, Fasoli M, Farina L, Anesi A, Guzzo F, Delledonne M, Pezzotti M (2013) The plasticity of the grapevine berry transcriptome. Genome Biol 14: r54
  Google Scholar: Author Only Title Only Author and Title

Dal Santo S, Zenoni S, Sandri M, De Lorenzis G, Magris G, De Paoli E, Di Gaspero G, Del Fabbro C, Morgante M, Brancadoro L, Grossi D, Fasoli M, Zuccolotto P, Tornielli GB, Pezzotti M (2018) Grapevine field experiments reveal the contribution of genotype, the influence of environment and the effect of their interaction (GxE) on the berry transcriptome. Plant J 93: 1143-1159
  Google Scholar: Author Only Title Only Author and Title

Fasoli M, Dal Santo S, Zenoni S, Tornielli GB, Farina L, Zamboni A, Porceddu A, Venturini L, Bicego M, Murino V, Ferrarini A, Delledonne M, Pezzotti M (2012) The grapevine expression atlas reveals a deep transcriptome shift driving the entire plant into a maturation program. Plant Cell 24: 3489-3505
  Google Scholar: Author Only Title Only Author and Title

Fasoli M, Richter CL, Zenoni S, Bertini E, Vitulo N, Dal Santo S, Dokoozlian N, Pezzotti M, Tornielli GB (2018) Timing and Order of the Molecular Events Marking the Onset of Berry Ripening in Grapevine. Plant Physiol 178: 1187-1206
  Google Scholar: Author Only Title Only Author and Title

Gildor T, Smadar BD (2018) Comparative Studies of Gene Expression Kinetics: Methodologies and Insights on Development and Evolution. Front Genet 9: 339
  Google Scholar: Author Only Title Only Author and Title

Gillaspy G, Ben-David H, Gruissem W (1993) Fruits: A Developmental Perspective. Plant Cell 5: 1439-1451
  Google Scholar: Author Only Title Only Author and Title

Hernández-Montes E, Zhang Y, Chang B-M, Shcherbatyuk N, Keller M (2021) Soft, Sweet, and Colorful: Stratified Sampling Reveals Sequence of Events at the Onset of Grape Ripening. American Journal of Enology and Viticulture 72: 137-151

Google Scholar: Author Only Title Only Author and Title

Hess M, Barralis, G., Bleiholder, H., Buhr, L., Eggers, TH., Hack, H., Stauss, R. (1997) Use of the extended BBCH scale - general for the descriptions of the growth stages of mono- and dicotyledonous weed species. Weed Research 37: 8
Google Scholar: Author Only Title Only Author and Title

Janssen BJ, Thodey K, Schaffer RJ, Alba R, Balakrishnan L, Bishop R, Bowen JH, Crowhurst RN, Gleave AP, Ledger S, McArtney S, Pichler FB, Snowden KC, Ward S (2008) Global gene expression analysis of apple fruit development from the floral bud to ripe fruit. BMC Plant Biol 8: 16
Google Scholar: Author Only Title Only Author and Title

Jolliffe IT (1986) Principal component analysis. Springer, New York, NY
Google Scholar: Author Only Title Only Author and Title

Kudoh H (2016) Molecular phenology in plants: in natura systems biology for the comprehensive understanding of seasonal responses under natural environments. New Phytol 210: 399-412
Google Scholar: Author Only Title Only Author and Title

Labadie M, Denoyes B, Guedon Y (2019) Identifying phenological phases in strawberry using multiple change-point models. J Exp Bot 70: 5687-5701
Google Scholar: Author Only Title Only Author and Title

Leiboff S, Hake S (2019) Reconstructing the Transcriptional Ontogeny of Maize and Sorghum Supports an Inverse Hourglass Model of Inflorescence Development. Current Biology 29: 3410-+
Google Scholar: Author Only Title Only Author and Title

Lorenz DH, Eichhorn KW, Bleiholder H, Klose R, Meier U, Weber E (1995) Growth Stages of the Grapevine: Phenological growth stages of the grapevine (Vitis vinifera L. ssp. vinifera)-Codes and descriptions according to the extended BBCH scale. Grape and wine research 1: 100-103
Google Scholar: Author Only Title Only Author and Title

Massonnet M, Fasoli M, Tornielli GB, Altieri M, Sandri M, Zuccolotto P, Paci P, Gardiman M, Zenoni S, Pezzotti M (2017) Ripening Transcriptomic Program in Red and White Grapevine Varieties Correlates with Berry Skin Anthocyanin Accumulation. Plant Physiol 174: 2376-2396
Google Scholar: Author Only Title Only Author and Title

Menzel A, Sparks TH, Estrella N, Koch E, Aasa A, Ahas R, Alm-KÜBler K, Bissolli P, BraslavskÁ OG, Briede A, Chmielewski FM, Crepinsek Z, Curnel Y, Dahl Å, Defila C, Donnelly A, Filella Y, Jatczak K, MÅGe F, Mestre A, Nordli Ø, PeÑUelas J, Pirinen P, RemiŠOvÁ V, Scheifinger H, Striz M, Susnik A, Van Vliet AJH, Wielgolaski F-E, Zach S, Zust ANA (2006) European phenological response to climate change matches the warming pattern. Global Change Biology 12: 1969-1976
Google Scholar: Author Only Title Only Author and Title

Meyer DH, Schumacher B (2021) BiT age: A transcriptome-based aging clock near the theoretical limit of accuracy. Aging Cell 20
Google Scholar: Author Only Title Only Author and Title

Nagano AJ, Kawagoe T, Sugisaka J, Honjo MN, Iwayama K, Kudoh H (2019) Annual transcriptome dynamics in natural environments reveals plant seasonal adaptation. Nat Plants 5: 74-83
Google Scholar: Author Only Title Only Author and Title

Nagano AJ, Sato Y, Mihara M, Antonio BA, Motoyama R, Itoh H, Nagamura Y, Izawa T (2012) Deciphering and prediction of transcriptome dynamics under fluctuating field conditions. Cell 151: 1358-1369
Google Scholar: Author Only Title Only Author and Title

Nissanka SP, Karunaratne AS, Perera R, Weerakoon WMW, Thorburn PJ, Wallach D (2015) Calibration of the phenology sub-model of APSIM-Oryza: Going beyond goodness of fit. Environmental Modelling & Software 70: 128-137
Google Scholar: Author Only Title Only Author and Title

Pagliarani C, Boccacci P, Chitarra W, Cosentino E, Sandri M, Perrone I, Mori A, Cuozzo D, Nerva L, Rossato M, Zuccolotto P, Pezzotti M, Delledonne M, Mannini F, Gribaudo I, Gambino G (2019) Distinct Metabolic Signals Underlie Clone by Environment Interplay in "Nebbiolo" Grapes Over Ripening. Front Plant Sci 10: 1575
Google Scholar: Author Only Title Only Author and Title

Parker AK, De CortÁZar-Atauri IG, Van Leeuwen C, Chuine I (2011) General phenological model to characterise the timing of flowering and veraison of Vitis vinifera L. Australian Journal of Grape and Wine Research 17: 206-216
Google Scholar: Author Only Title Only Author and Title

Parker AK, García de Cortázar-Atauri I, Gény L, Spring J-L, Destrac A, Schultz H, Molitor D, Lacombe T, Graça A, Monamy C, Stoll M, Storchi P, Trought MCT, Hofmann RW, van Leeuwen C (2020) Temperature-based grapevine sugar ripeness modelling for a wide range of Vitis vinifera L. cultivars. Agricultural and Forest Meteorology 285-286
Google Scholar: Author Only Title Only Author and Title

Parker AK, Hofmann RW, van Leeuwen C, McLachlan ARG, Trought MCT (2015) Manipulating the leaf area to fruit mass ratio alters the synchrony of total soluble solids accumulation and titratable acidity of grape berries. Australian Journal of Grape and Wine Research 21: 266-276
Google Scholar: Author Only Title Only Author and Title

Pastore C, Dal Santo S, Zenoni S, Movahed N, Allegro G, Valentini G, Filippetti I, Tornielli GB (2017) Whole Plant Temperature Manipulation Affects Flavonoid Metabolism and the Transcriptome of Grapevine Berries. Front Plant Sci 8: 929
Google Scholar: Author Only Title Only Author and Title

Rabut C (2002) On Pierre Bezier's life and motivations. Computer-Aided Design 34: 493-510
Google Scholar: Author Only Title Only Author and Title

Robinson S, Glonek G, Koch I, Thomas M, Davies C (2015) Alignment of time course gene expression data and the classification of developmentally driven genes with hidden Markov models. BMC Bioinformatics 16: 196
Google Scholar: Author Only Title Only Author and Title

Sadras VO, Moran MA (2012) Elevated temperature decouples anthocyanins and sugars in berries of Shiraz and Cabernet Franc. Australian Journal of Grape and Wine Research 18: 115-122
Google Scholar: Author Only Title Only Author and Title

Sanchez-Sevilla JF, Vallarino JG, Osorio S, Bombarely A, Pose D, Merchante C, Botella MA, Amaya I, Valpuesta V (2017) Gene expression atlas of fruit ripening and transcriptome assembly from RNA-seq data in octoploid strawberry (Fragaria x ananassa). Sci Rep 7: 13737
Google Scholar: Author Only Title Only Author and Title

Shinozaki Y, Nicolas P, Fernandez-Pozo N, Ma Q, Evanich DJ, Shi Y, Xu Y, Zheng Y, Snyder SI, Martin LBB, Ruiz-May E, Thannhauser TW, Chen K, Domozych DS, Catala C, Fei Z, Mueller LA, Giovannoni JJ, Rose JKC (2018) High-resolution spatiotemporal transcriptome mapping of tomato fruit development and ripening. Nat Commun 9: 364
Google Scholar: Author Only Title Only Author and Title

Theine J, Holtgrawe D, Herzog K, Schwander F, Kicherer A, Hausmann L, Viehover P, Topfer R, Weisshaar B (2021) Transcriptomic analysis of temporal shifts in berry development between two grapevine cultivars of the Pinot family reveals potential genes controlling ripening time. BMC Plant Biol 21: 327
Google Scholar: Author Only Title Only Author and Title

Wang C, Han J, Shangguan L, Yang G, Kayesh E, Zhang Y, Leng X, Fang J (2014) Depiction of Grapevine Phenology by Gene Expression Information and a Test of its Workability in Guiding Fertilization. Plant Molecular Biology Reporter 32: 1070-1084
Google Scholar: Author Only Title Only Author and Title

Wickham H (2009) Ggplot2: Elegant Graphics for Data Analysis, Ed 2nd Edition. Springer
Google Scholar: Author Only Title Only Author and Title